Supporting information

Highly Efficient Electrocatalyst for the Oxygen Reduction Reaction: Phosphorus and Nitrogen Co-Doped Ordered Porous Carbon derived from an Iron-Functionalized Mesoporous Polymer

Chengwei Deng,[a,b] Hexiang Zhong,[a,*] Xianfeng Li,[a,c] Lan Yao,[a,b] and Huamin Zhang[a,c,*]

[a] Division of Energy Storage, Dalian National Laboratory for Clean Energy (DNL)
Dalian Institute of Chemical Physics, Chinese Academy of Sciences
Dalian 116023, China

[b] Graduate University of the Chinese Academy of Sciences
Beijing 100049, China

[c] Collaborative Innovation Centre of Chemistry for Energy Materials (iChEM), Dalian 116023 (P.R. China)

Corresponding authors:
zhanghm@dicp.ac.cn; zhonghexiang@dicp.ac.cn

Supplementary Tables and Figures

1. Textural parameters of the prepared catalysts

Table S1 shows the textural parameters of the three prepared catalysts obtained using a Micromeritics ASAP 2020 surface area and porosity analyzer. As shown, the BET surface area and the pore volume of NHOPC are larger than those of PHOPC. This result indicates that the nitridation process can greatly increase the surface area and the pore volume. Furthermore, the BET surface area and pore volume of PNHOPC are increased compared to those of NHOPC, which suggests that the P species can change the surface area and pore volume.

Table S1. Textural Parameters of PNHOPC, NHOPC and PHOPC**.**

Sample	BET surface area ($m^2\ g^{-1}$) [a,b]	Pore size diameters (nm) [c]	Total pore volume ($cm^3\ g^{-1}$)
PNHOPC	1118	4.1	1.1403
PHOPC	448	3.4	0.3826
NHOPC	903	3.3	0.7364

[a] BET was obtained in the range of 0.01-0.05 P/P_0.

[b] Total pore volumes calculated as the amount of N_2 adsorbed at a relative pressure of 0.974.

[c] Calculated from the N_2 desorption branch of the isotherms by the BJH method.

2. Surface composition and the concentrations of different N groups

In Table S2, the surface concentrations of C, N, P, O, Fe and different nitrogen species in PNHOPC, NHOPC and PHOPC are listed. For NHOPC, the surface nitrogen concentration and iron concentration are 4.45 atomic% and 0.33 atomic%. The nitrogen content in PNHOPC (3.32%) is lower than that in NHOPC. The concentrations of phosphorous in PHOPC and PNHOPC are 0.22% and 0.16%, respectively.

As shown in Table S2, the N 1s XPS spectrum was deconvoluted into four peaks: pyridinic N, pyrrolic N, graphitic N and N-oxide compounds [1]. The concentrations of pyridinic-N and graphitic-N in NHOPC and PNHOPC are similar. However, PNHOPC shows an intense Fe-N peak compared with that of NHOPC. This result suggests that the pyridinic N and graphitic N significantly contribute to the ORR catalytic activity and that graphitic N can be more effective than pyridinic N and other N species for enhancing the ORR activity.

Table S2. Surface Composition and the Concentrations of Different N groups in the Prepared Catalysts.

Samples	**Surface Composition (atomic %)**					**Concentrations of different N groups (atomic %)**			
	Carbon	Nitrogen	Oxygen	Iron	Phosphors	Pyridinic N	Pyrrolic N	Graphitic N	N-O
PNHOPC	89.09	3.32	7.02	0.41	0.16	40.53	20.79	35.73	2.94
NHOPC	86.91	4.45	8.25	0.33	/	34.83	30.27	24.34	10.56
PHOPC	92.13	/	7.25	0.40	0.22	/	/	/	/

3. Comparison of ORR performance in acidic media for PNHOPC and other non-noble metal ORR electrocatalysts

In order to obtain meaningful current densities from the reduction of oxygen, the kinetics of the ORR must be increased by lowering the activation energy of the reaction. The activation energy is lowered through the use of electrocatalysts and also by reducing the electrode potential. The difference between the electrode potential (E) and the equilibrium potential (E_{eq}, 1.23 V for the ORR) of the electrode reaction is known as the over potential, η (Equation 3.1).

$$\eta = E - E_{eq} \tag{3.1}$$

The ORR performances in acidic media for PNHOPC and other non-noble metal ORR electrocatalysts are compared by comparing the over potential of the ORR at three given current densities (0.5 mA/cm^2, 1 mA/cm^2, 2 mA/cm^2). Commercially obtained Pt/C (20 wt. %, JM Co.) was also examined under the same conditions for comparison. The results are shown in Table S3. The PNHOPC is highly active toward the ORR and it can generate a current density of 1 mA cm^{-2} at an over potential of 440 mV, which is comparable to the PANI-Fe-C[2] reported in Science.

Table S3. Comparison of ORR performance in acidic media for the PNHOPC and other non-noble metal ORR electrocatalysts.

Catalyst	Over potential at the Current density j = 0.5 mA/cm^2 (mV)	Over potential at the Current density j = 1 mA/cm^2 (mV)	Over potential at the Current density j = 2 mA/cm^2 (mV)	Reference
Pt/C (20 wt. %, JM Co.)	350	375	404	This work
PNHOPC	410	440	478	
Fe_3C/NG-800[3]	420	432	470	Adv Mater 2015, 27, 2521-2527
CPANI-Fe-NaCl[4]	425	470	505	J Am Chem Soc 2015, 137, 5414-5420.
Co-N/MWCNT-2[5]	490	530	630	Journal of Power Sources 2015, 278, 296-307.
Fe_3C/C-700[6]	470	480	530	Angew Chem Int Ed Engl 2014, 53, 3675-3679.
NGCA[7]	450	480	540	Applied Catalysis B: Environmental 2014, 144, 760-766.
Fe-N-C-700[8]	505	535	610	Carbon 2013, 57, 443-451.
NC-750[9]	678	803	1068	Carbon 2012, 50, 2620-2627.
Fe-N-rGO[10]	490	530	600	Chemistry of Materials 2011, 23, 3421-3428.
Fe–N-MWCNTs[11]	470	500	560	Phys Chem Phys 2011, 13, 21437-21445. 153.
PANI-Fe-C[2]	360	405	430	Science 2011, 332, 443-447.
NPMC-900[12]	460	505	526	Journal of Power Sources 2010, 195, 6373-6378.

4. XPS-C 1S spectroscopy of the prepared catalysts

As shown in Figure S1, the binding energy of NHOPC is up-shifted by 0.15 eV compared to that of bare graphite (284.5 eV), suggesting that electrons of the C atoms are transferred to the doped N atoms. PHOPC shows the C-C bond peak at 284.59 eV, which is 0.09 eV higher than that of bare graphite. For PNHOPC, the C-C bond peak is up-shifted by 0.25 eV due to the charge delocalization caused by N-doping and P-doping.

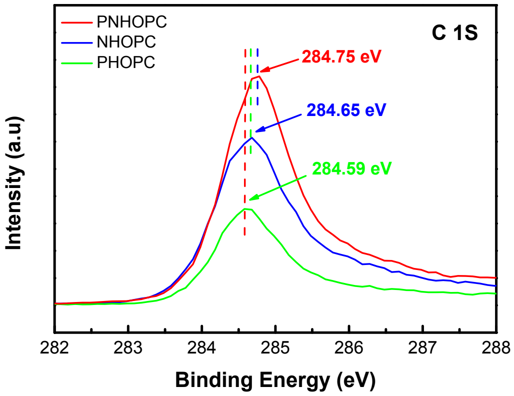

Figure S1. C1S XPS spectra of the prepared catalysts.

5. Methanol tolerance of the PNHOPC and Pt/C catalysts

Figure S2 shows the liner sweep voltammetry results for the PNHOPC and Pt/C catalysts. In a methanol-free oxygen-saturated electrolyte, the PNHOPC and Pt/C catalysts show high activity for the ORR. However, the results are markedly different after 0.5 M methanol is added. As shown in Figure S2a, PNHOPC retains the same initial onset potential for the ORR, and the current density at 0.75 V is approximately 100% of that obtained in methanol-free electrolyte. These results demonstrate the outstanding methanol tolerance of the PNHOPC catalyst. In contrast, the ORR density of the Pt/C catalyst decreases after the addition of 0.5 M methanol, and the methanol oxidation reaction (MOR) peak occurs at approximately 0.70 V. The ORR and MOR occur simultaneously on the surface of the Pt/C catalyst, which indicates the poor methanol tolerance of the Pt/C catalyst. Moreover, it can be observed that the ORR onset potential decreased for Pt/C.

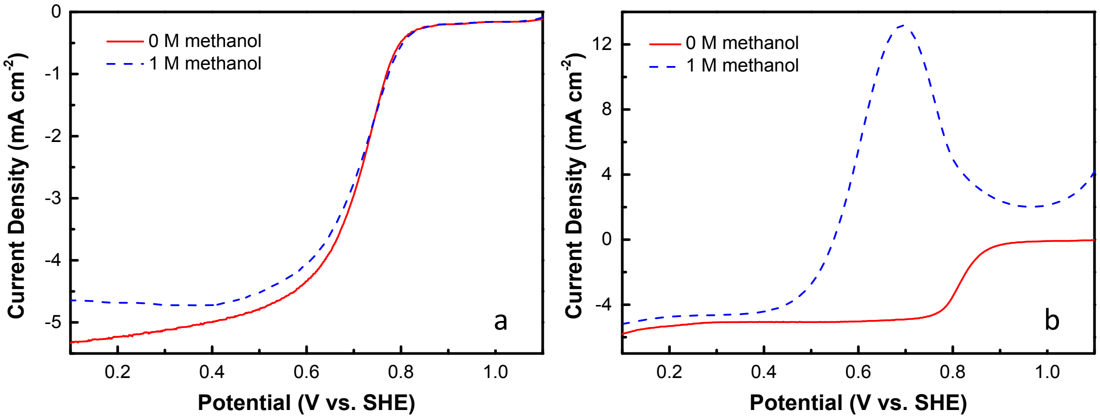

F

igure S2. ORR activities of (a) PNHOPC and (b) Pt/C Pt/C in O_2-saturated 0.5 M H_2SO_4 with and without 1 M methanol at a rotation rate of 1600 rpm.

6. ORR activity of the Pt/C and PNHOPC in $HClO_4$

Figure S3 shows the liner sweep voltammetry results for the PNHOPC and Pt/C catalysts in O_2-saturated 1 M $HClO_4$. As shown in Figure S3, the PNHOPC catalyst excellent ORR catalytic activity with the onset potential of 0.99 V and the limiting diffusion current of 5.56 mA cm^{-2}. For the Pt/C, the onset potential is 1.0 V, and the limiting diffusion current is 4.86 mA cm^{-2}.

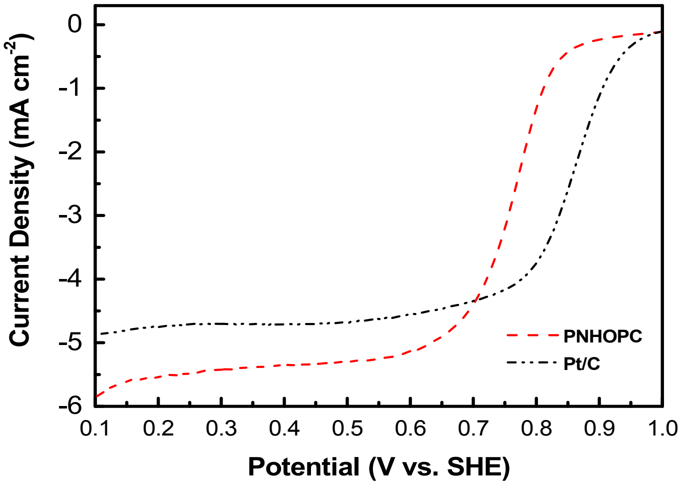

Figure S3. ORR activities of (a) PNHOPC and (b) Pt/C Pt/C in O_2-saturated 1 M $HClO_4$ at a rotation rate of 1600 rpm.

[1] aH. Peng, Z. Mo, S. Liao, H. Liang, L. Yang, F. Luo, H. Song, Y. Zhong, B. Zhang, *Scientific reports* **2013**, *3*, 1765; bL. Lai, J. R. Potts, D. Zhan, L. Wang, C. K. Poh, C. Tang, H. Gong, Z. Shen, J. Lin, R. S. Ruoff, *Energy & Environmental Science* **2012**, *5*, 7936-7942.
[2] G. Wu, K. L. More, C. M. Johnston, P. Zelenay, *Science* **2011**, *332*, 443-447.
[3] M. Xiao, J. Zhu, L. Feng, C. Liu, W. Xing, *Adv Mater* **2015**, *27*, 2521-2527.
[4] W. Ding, L. Li, K. Xiong, Y. Wang, W. Li, Y. Nie, S. Chen, X. Qi, Z. Wei, *J Am Chem Soc* **2015**, *137*, 5414-5420.
[5] L. Osmieri, A. H. A. Monteverde Videla, S. Specchia, *Journal of Power Sources* **2015**, *278*, 296-307.
[6] Y. Hu, J. O. Jensen, W. Zhang, L. N. Cleemann, W. Xing, N. J. Bjerrum, Q. Li, *Angew Chem Int Ed Engl* **2014**, *53*, 3675-3679.
[7] C. H. Choi, M. W. Chung, H. C. Kwon, J. H. Chung, S. I. Woo, *Applied Catalysis B: Environmental* **2014**, *144*, 760-766.
[8] H. Xiao, Z.-G. Shao, G. Zhang, Y. Gao, W. Lu, B. Yi, *Carbon* **2013**, *57*, 443-451.
[9] Z. Mo, S. Liao, Y. Zheng, Z. Fu, *Carbon* **2012**, *50*, 2620-2627.
[10] H. R. Byon, J. Suntivich, Y. Shao-Horn, *Chemistry of Materials* **2011**, *23*, 3421-3428.
[11] H. R. Byon, J. Suntivich, E. J. Crumlin, Y. Shao-Horn, *Phys Chem Chem Phys* **2011**, *13*, 21437-21445.
[12] X. Li, G. Liu, B. N. Popov, *Journal of Power Sources* **2010**, *195*, 6373-6378.